

Neutron diffraction investigations of zero-field and field-induced magnetic structures of DyNiSn single crystal

K. Murogaki^{a,*}, S. Kawano^b, Y. Andoh^c, M. Takahashi^d, M. Kurisu^e,
G. Nakamoto^e, D.T. Kim Anh^e, T. Tsutaoka^f

^a Graduate School of Science, Kyoto University, Kyoto 606-8502, Japan

^b Research Reactor Institute, Kyoto University, Osaka 590-0494, Japan

^c Faculty of Regional Sciences, Tottori University, Tottori 680-8551, Japan

^d Institute of Materials Science, University of Tsukuba, Ibaraki 305-8573, Japan

^e Japan Advanced Institute of Science and Technology, Ishikawa 923-1292, Japan

^f Graduate School of Education, Hiroshima University, Hiroshima 739-8524, Japan

Available online 13 January 2006

Abstract

Single crystal neutron diffraction studies have been performed on the rare-earth ternary compound, DyNiSn. This crystal exhibits an incommensurate magnetic structure expressed by the propagation vector, $\mathbf{Q} = (0.662\ 0.352\ 0)$ with its third harmonics at low temperatures. In an external magnetic field applied along the c -axis DyNiSn shows incommensurate modulation with $\mathbf{Q} = (1\ 0.315\ 0)$ at 1.6 K, while along the easy magnetization direction of the b -axis a commensurate modulation with $\mathbf{Q} = (2/3\ 0\ 0)$ develops at 2 K. The results along the b -axis are fully consistent with the magnetization curve.

© 2005 Published by Elsevier B.V.

Keywords: Magnetically ordered materials; DyNiSn; Neutron scattering; Diffraction; Magnetic structure

1. Introduction

Ternary equiatomic rare-earth compound DyNiSn crystallizes in the orthorhombic TiNiSi-type structure (space group: $Pnma$) [1]. Only the Dy atoms bear the magnetic moment and occupy the 4(c) sites of the chemical cell. The magnetic properties of DyNiSn are characterized by the temperature-induced successive magnetic transitions at $T_N = 7.3$ K and $T_1 = 5.4$ K and the multi-step (three steps) metamagnetic transitions at low temperatures when the magnetic field is applied along the easy magnetization direction of the b -axis [2]. Szytula et al. have reported a sine-modulated structure with the magnetic wave vector of $\mathbf{Q} = (Q_x\ Q_y\ 0)$ type at $T = 2$ K from the powder neutron diffraction measurements [3], while Kawano et al. have recently reported that the zero-field magnetic structure is expressed by $\mathbf{Q} = (0.641\ 0.340\ 0)$

at low temperatures from the single crystal neutron diffraction measurements [4]. They have also studied the magnetic structures of an iso-structural compound TbNiSn and found a similar magnetic structure with $\mathbf{Q} = (0.600\ 0.345\ 0)$ at low temperatures [4]. Furthermore, they have observed a new intermediate phase with $\mathbf{Q} = (2/3\ 0\ 0)$ to develop in an external magnetic field for the low temperature phase of TbNiSn. In the present note, we report more detailed results of neutron diffraction studies of not only zero-field structure but also field-induced structure of a DyNiSn single crystal and propose possible magnetic structures for the observed phases in which the antiferromagnetic modulations are mostly incommensurate.

2. Experimental details

Dysprosium (purity 99.9%), nickel (purity 99.99%) and tin shots (purity 99.99%) were used as starting materials. The polycrystalline ingots were prepared by arc-melting the

* Corresponding author. Present address: MHI Kobe Takamaru Dormitory, Kobe 655-0016, Japan.

E-mail address: murogaki@fiberbit.net (K. Murogaki).

mixtures of the starting materials at the equiatomic ratio in a purified argon atmosphere. Then, a single crystal was grown by the Czochralski method using a tri-arc furnace. The pulsed-neutron diffraction measurements were performed in the a^*-b^* reciprocal plane for the field-induced phases at low temperatures using the KENS-FOX diffractometer in Tsukuba, Japan. The reactor-based neutron measurements were carried out in the a^*-b^* and a^*-c^* reciprocal planes for the field-induced phases at low temperatures with the KUR-TAS using 1.006 Å incident neutrons installed at the Kyoto University Reactor (KUR) in Kumatori, Japan. The magnetic field is applied along the b -axis of the easy magnetization direction for the a^*-c^* plane and the c -axis of a hard magnetization direction for the a^*-b^* reciprocal plane, respectively.

3. Results and discussion

3.1. Zero-field phases

Fig. 1 shows the distribution of pulsed-neutron intensities in the a^*-b^* reciprocal plane for the low temperature phase below $T_1 = 5.4$ K. There appear magnetic reflections at $(h \pm 0.662, k \pm 0.352, 0)$ for the nuclear reflections containing the large Dy structure factors. Therefore, the magnetic wave vector is determined to be $\mathbf{Q} = (0.662, 0.352, 0)$.

Fig. 2 gives a schematic representation of the Bragg reflections in the a^*-c^* reciprocal plane at $T = 1.84$ K. The weak reflections were found at $\mathbf{Q} = (h \pm q_1, 0, l)$ with $q_1 = 0.08a^*$ for $h+l = \text{odd}$, but there was no magnetic reflection on the a^* -axis. These weak satellites observed in the a^*-c^* plane are considered to be the third satellites from the main satellites in the a^*-b^* plane, for instance $(0.08, 0, 1)$ appears as the third harmonics of the $(1.338, 0.648, 1)$ and $(1.338, -0.648, 1)$ main satellites. Considering that the magnetic reflections in the a^*-c^* plane come from the main satellites in the a^*-b^*

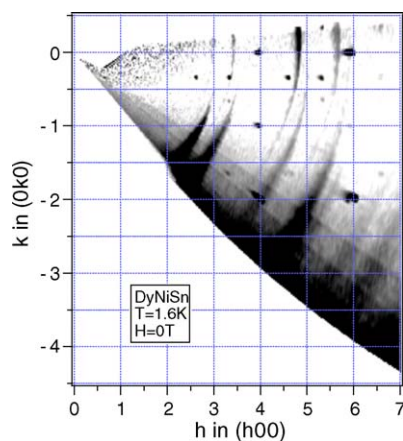


Fig. 1. Distribution of pulsed-neutron intensities in the a^*-b^* reciprocal plane at $T = 1.6$ K for DyNiSn single crystal. Broad arcs in the figure indicate Debye–Scherrer rings of scattering from an Al cryostat.

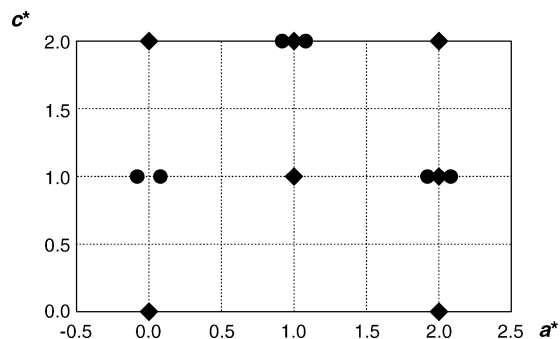


Fig. 2. Schematic representation of Bragg reflections in the a^*-c^* reciprocal plane at 1.84 K, (●) magnetic reflections and (◆) nuclear reflections.

plane, one can understand that there is no magnetic reflection on the a^* -axis in the a^*-c^* plane, although the easy axis of magnetization is the b -axis.

The antiferromagnetic to paramagnetic transition temperature is determined to be 6.5 K by the temperature dependence of the peak height intensity of the $(0.662, 0.352, 0)$ main satellite as shown in Fig. 3. The temperature dependence of the $(0.08, 0, 1)$ satellite shows a linear decrease with increasing temperature, which is a typical thermal behaviour of higher harmonics components around the critical temperature. On the other hand, the intensity at $(0.662, 0.352, 0)$ shows an abrupt decrease around $T = 6.5$ K. Any transition is not observed other than the one around $T = 6.5$ K in the present study. Thus, the Neel temperature is identified to be $T_N = 6.5$ K.

The Dy atom is very absorptive to thermal neutrons in the compound. Our single crystal is very anisotropic in shape for the neutron path in this experimental arrangement, so that the neutron path for the $(0.662, 0.352, 0)$ satellite measurement is longer, while that for the $(0.08, 0, 1)$ satellite is shorter. Therefore, the comparable intensities between the first and third magnetic satellites can be interpreted. Thus, the magnetic structure is expressed by the incommensurate $\mathbf{Q} = (0.662, 0.352, 0)$ and its third harmonics. An approximated magnetic structure in this phase is illustrated in Fig. 4.

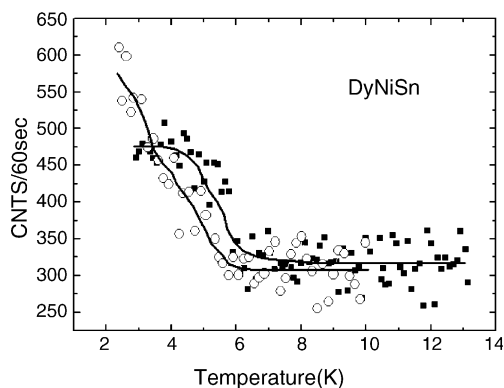


Fig. 3. Temperature dependence of the peak height intensities of the first and third satellites for DyNiSn, (■) $(0.662, 0.352, 0)$ main satellite and (○) $(0.08, 0, 1)$ third satellite. The lines are guide to eye.

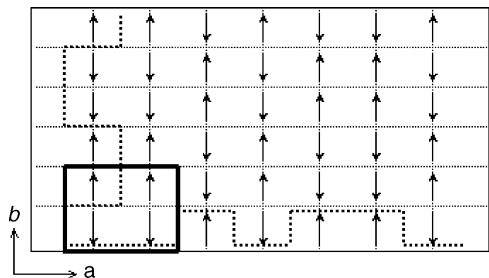


Fig. 4. Approximated representation of a squared incommensurate magnetic structure with $Q = (0.662\ 0.352\ 0)$. The bold frame denotes the chemical unit cell.

3.2. Field-induced phases

3.2.1. Case of field parallel to the c -axis

Fig. 5 shows the diffraction pattern for the field-induced phase in the a^*-b^* reciprocal plane in $H = 2.5$ T at 1.6 K. Refer to the previous bulk magnetization measurement at 1.6 K indicating the two metamagnetic transitions along the c -axis at $H = 2.0$ and 3.4 T [2].

At the field of $H = 2.5$ T applied along the c -axis, the zero-field magnetic Bragg reflections disappear and new reflections appear. The field-induced phase is assigned by $Q = (1\ 0.315\ 0)$ and persist in the range of $H = 2.5$ –4.0 T. Any change is not observed in the diffraction patterns at the critical field of 3.4 T in the present measurements.

Fig. 6 gives the field dependence of the $(0.662\ 0.352\ 0)$ reflection at $T = 2.18$ K, when the magnetic field is applied along the c -axis. An abrupt decrease is observed around $H = 1.6$ T. An approximated magnetic structure described by $Q = (1\ 1/3\ 0)$ is shown in Fig. 7.

3.2.2. Case of field parallel to the b -axis

On the other hand, when the field is applied along the easy magnetization direction of the b -axis, the zero-field magnetic Bragg reflections disappear and new reflections assigned by

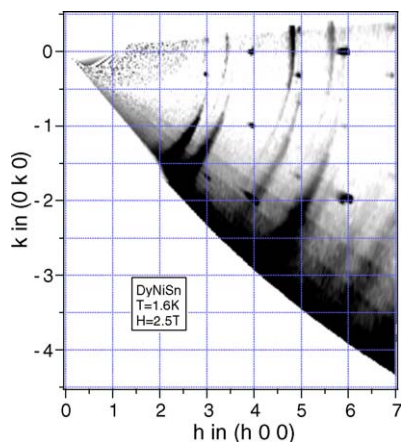


Fig. 5. Distribution of pulsed-neutron intensities in the a^*-b^* reciprocal plane in $H = 2.5$ T along the c -axis at $T = 1.6$ K for DyNiSn single crystal. Broad arcs in the figure indicate Debye-Scherrer rings of scattering from an Al cryostat.

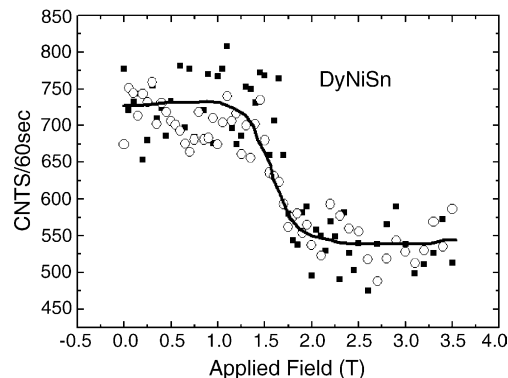


Fig. 6. Field dependence of the $(0.662\ 0.352\ 0)$ magnetic reflection for $H // c$ -axis at $T = 2.18$ K, (■) field increasing and (○) field decreasing. The line is guide to eye.

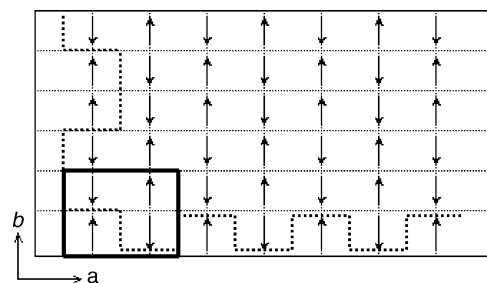


Fig. 7. Approximated representation of a squared incommensurate magnetic structure of the $Q = (1\ 0.315\ 0)$ phase. The bold frame denotes the chemical unit cell.

$Q = (2/3\ 0\ 0)$ appear in the a^*-c^* reciprocal plane as shown in Fig. 8. It is of particular interest to note that quite similar field dependence of the wave vector has been found in TbNiSn [4]. The $(0.08\ 0\ 1)$ reflection disappears above 0.6 T, and induced ferromagnetic components are gradually developing on the nuclear reflections. Furthermore, new magnetic reflections appear at $(2/3\ 0\ 0)$ and these reflections disappear at 1.2 T with

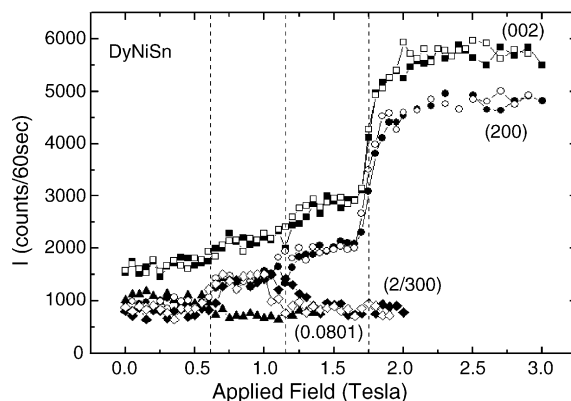


Fig. 8. Magnetic field dependence of representative magnetic reflections in the a^*-c^* reciprocal plane at 2.0 K. Magnetic field is applied along the b -axis of the easy magnetization axis, (■, □) (002) ; (●, ○) (200) ; (◆, ◇) $(2/300)$ and (▲) $(0.08\ 0\ 1)$. The open and filled symbols denote the cases of field increasing and decreasing, respectively.

further increasing field. Between 0.6 and 1.2 T the $(2/3\ 0\ 0)$ reflection takes constant value. The ferromagnetic components increase rapidly at 1.75 T to approach its full moment with further increasing field. One can, thus, obtain the following four metamagnetic phases: (1) in $0 < H < 0.6$ T, the magnetic structure is described by $\mathbf{Q} = (0.662\ 0.352\ 0)$ and its third harmonics as shown in Fig. 4; (2) in $0.6\ \text{T} < H < 1.2$ T, the magnetic structure described by the $2\bar{1}$ sequence of ferromagnetic planes perpendicular to the a -axis, where ‘ n ’ and ‘ \bar{n} ’ denote n consecutive ferromagnetic planes parallel and antiparallel to the magnetic field, respectively; (3) in $1.2\ \text{T} < H < 1.75$ T, the $(2/3\ 0\ 0)$ reflection disappears and (4) in $1.75\ \text{T} < H$, the ferromagnetic component reaches its full moment.

4. Conclusions

We have determined the zero-field magnetic structure of DyNiSn to be expressed by the magnetic wave vector $\mathbf{Q} = (0.662\ 0.352\ 0)$ and its higher harmonics below T_N . When the magnetic field is applied along the hard magnetization direction of the c -axis up to 4.0 T, an intermediate phase described by the incommensurate $\mathbf{Q} = (1\ 0.315\ 0)$ with induced ferromagnetic components appears. On the other hand, in the case of field parallel to the easy magnetization

direction of the b -axis the intermediate phase with the commensurate $\mathbf{Q} = (2/3\ 0\ 0)$ and induced ferromagnetic components develops. The field dependence of the magnetic intensities is fully consistent with the previous bulk magnetization measurements [2]. The determined magnetic structures for the field-induced phases for DyNiSn are found to be very similar to those of TbNiSn [4].

Acknowledgments

The reactor-based neutron and the pulsed-neutron experiments were supported in part by the Visiting Research Programs of Kyoto University Research Reactor Institute (KURRI) at Kumatori, Japan, and by the Visiting Research Program of High Energy Accelerator Research Organization at Tsukuba, Japan, respectively.

References

- [1] A.E. Dwight, *J. Less-Common Met.* 93 (1983) 411.
- [2] M. Kurisu, H. Hori, M. Furusawa, M. Miyake, Y. Andoh, I. Oguro, K. Kindo, T. Takeuchi, A. Yamagishi, *Physica B* 201 (1994) 107.
- [3] A. Szytula, B. Penc, E. Ressouche, *J. Alloys Compd.* 244 (1996) 94.
- [4] S. Kawano, Y. Andoh, M. Kurisu, *J. Phys. Chem. Solids* 60 (1999) 1205.